Compact Saloplastic Poly(Acrylic Acid)/Poly(Allylamine) Complexes: Kinetic Control Over Composition, Microstructure, and Mechanical Properties

Andreas Reisch, Patricia Tirado, Emilie Roger, Fouzia Boulmedais, Dominique Collin, Jean-Claude Voegel, Benoît Frisch, Pierre Schaaf, and Joseph B. Schlenoff*

Durable compact polyelectrolyte complexes (CoPECs) with controlled porosity and mechanical properties are prepared by ultracentrifugation. Because the starting materials, poly(allylamine hydrochloride) (PAH) and poly(acrylic acid sodium salt) (PAA), are weak acids/bases, both composition and morphology are controlled by solution pH. In addition, the nonequilibrium nature of polyelectrolyte complexation can be exploited to provide a range of compositions and porosities under the influence of polyelectrolyte addition order and speed, and concentration. Confocal microscopy shows these "saloplastic" materials to be highly porous, where pore formation is attributed to a combination of deswelling of the polyelectrolyte matrix and expansion of small inhomogenities by osmotic pressure. The porosity (15–70%) and the pore size (<5 μm to >70 μm) of these materials can be tuned by adjusting the PAA to PAH ratio, the salt concentration, and the pH. The modulus of these CoPECs depends on the ratio of the two polyelectrolytes, with stoichiometric complexes being the stiffest due to optimized charge pairing, which correlates with maximized crosslinking density. Mechanical properties, pore sizes, and pore density of these materials make them well suited to three dimensional supports for tissue engineering applications.

1. Introduction

Functional materials for use in biological environments and biomedical applications, ranging from enzyme carriers or drug delivery systems to tissue engineering scaffolds, require hydration and often porosity to interact efficiently with their environments and allow the exchange of material (from small molecules to cells) and information (usually in the form of chemical signals).[1] Consequently, various types of porous matrices, especially hydrated polymeric materials as hydrogels, have attracted attention over the last half century.

Polyelectrolyte complexes are a versatile class of physical hydrogels which rely on physical cross-links formed by interactions between positively and negatively charged groups on polycations and polyanions. The main driving force for their formation is the entropy gain associated with the release of small counterions and hydration water,[2–4] this process is reversible and salt ions are able to break polyelectrolyte ion pairs in a process termed doping.[5]

Precipitation of individual polyelectrolytes and salt doping of the complex are shown respectively

$$Pol^{+}Cl^{-}_{aq} + Pol^{-}Na^{+}_{aq} \rightarrow Pol^{+}\,Pol_{s}{}^{-} + Na^{+}_{aq} + Cl^{-}_{aq} \rightarrow \text{precipitation} \quad (1.1)$$

$$Pol^{+}Pol_{s}{}^{-} + Na^{+}_{aq} + Cl^{-}_{aq} \rightarrow Pol^{+}\,Cl_{s}{}^{-} + Pol^{-}\,Na_{s}{}^{+} \rightarrow \text{salt doping} \quad (1.2)$$

where "aq" is the aqueous phase and "s" is the solid polyelectrolyte complex phase.

The morphology and applications of polyelectrolyte complexes depend on the polyelectrolytes used and the conditions under which they are combined: dilute solutions and a large excess of one of the polyelectrolytes leads to the formation of quasi-soluble complexes with applications in drug delivery.[6] Strongly hydrated polymers can yield liquid-like coacervates used in the food[7] and pharmaceutical industries.[8] Alternating deposition provides polyelectrolyte multilayers[9] with applications ranging from electronics and optics,[10] to biomedical devices[11,12] and stimuli responsive materials.[13,14] Solution precipitated polyelectrolyte complexes (PECs) are obtained

Dr. A. Reisch, P. Tirado, Dr. E. Roger, Dr. B. Frisch
Laboratoire de Conception et Application de Molécules Bioactives
UMR 7199, CNRS/Université de Strasbourg
Faculté de Pharmacie
74 route du Rhin, 67401 Illkirch Cedex
France, and International Center for Frontier Research in Chemistry
8 allée Gaspard Monge, 67083 Strasbourg, France
E-mail: frisch@unistra.fr
Dr. F. Boulmedais, Dr. D. Collin, Prof. P. Schaaf
Centre National de la Recherche Scientifique
Institut Charles Sadron
UPR 22, 23 rue du Loess
67034 Strasbourg Cedex
France, and International Center for Frontier Research in Chemistry
8 allée Gaspard Monge, 67083 Strasbourg, France.
Dr. J.-C. Voegel
Institut National de la Santé et de la Recherche Médicale
INSERM Unité 977, 11 rue Humann, 67085 Strasbourg Cedex, France.
Prof. J. B. Schlenoff
Department of Chemistry and Biochemistry
The Florida State University
Tallahassee, FL 32306, USA

DOI: 10.1002/adfm.201201413

by mixing roughly stoichiometric amounts of polyanions and polycations. Though easy to prepare, PECs are extremely difficult to process, as they are infusible and insoluble in most solvents.[2,15,16] Using ternary solvents Michaels and coworkers[15,16] were able to dissolve PECs and cast films of these materials. For decades, this remained the only processing technique for macroscopic PEC materials, thus restricting PECs mainly to membrane type applications. Recently Schlenoff and coworkers discovered that it is possible to plasticize complexes made of the strong polyelectrolytes poly(styrene sulfonate) (PSS) and poly(diallyldimethylammonium) (PDADMA) by doping with high concentrations of salt sufficiently to allow their compaction by ultracentrifugation[17,18] and their processing by extrusion,[19] leading to macroscopically homogeneous materials they termed compact polyelectrolyte complexes (CoPECs) with interesting mechanical properties resembling those of cartilage[18] or tendon.[19] In the present work we applied this new processing technique, ultracentrifugation in the presence of salt, to complexes of two weak polyelectrolytes, poly(acrylic acid) (PAA) and poly(allylamine hydrochloride) (PAH). Multilayers of these two polyelectrolytes have been extensively studied, especially as coatings for biomedical applications.[20–22] Their versatility is due to the possibility of tuning the charge density of the polyelectrolytes by pH. PECs made from PAA and PAH are not only responsive to salt concentration (Equation 1.2) but also to pH,[23–26] as shown in **Scheme 1**.

Mechanical properties, hydration, and structure of materials for biomedical applications not only determine macroscopic behavior and the exchange of matter, but also, together with their (bio)chemical composition, influence cell response.[27] The latter is of paramount interest for tissue engineering applications, where suitable microenvironments are used to direct cell behavior.[27] Various approaches have been developed to control properties in different types of materials: introduction of cross-links is used to tune mechanical properties, introduction of hydrophilic groups to adjust hydration. Pores can be created through induced phase separation[28,29] or the use of solid or gaseous porogens.[30,31] However, these approaches usually require multiple steps, including synthesis and/or processing. In this work, we will show that the influence of kinetic phenomena on PEC formation[32] offers convenient ways of controlling their properties and structure through straightforward variations of assembly conditions. Though individual ion pairs between charged groups on polyanions and polycations in PECs are under thermodynamic control as suggested by Equations (1) and (2), the cooperativity of interactions means longer chain segments can be kinetically trapped.[33] Even in the presence of high concentrations of salt the PEC cannot equilibrate quickly. In consequence, the way in which the polyelectrolytes encounter each other in solution becomes important for the formation of these materials, leading to kinetic control. As we will show this kinetic control can be used not only to determine the composition of the materials, but also to control their structure, porosity, pore size distribution, and mechanical properties.

2. Results and Discussion

Precipitates obtained by mixing PAA and PAH solutions could be compacted by ultracentrifugation, yielding macroscopically homogeneous materials with tough mechanical properties: CoPECs (**Figure 1**). During preliminary experiments it became clear that the appearance and stiffness of the CoPECs depended on the precise way in which the solutions were mixed.

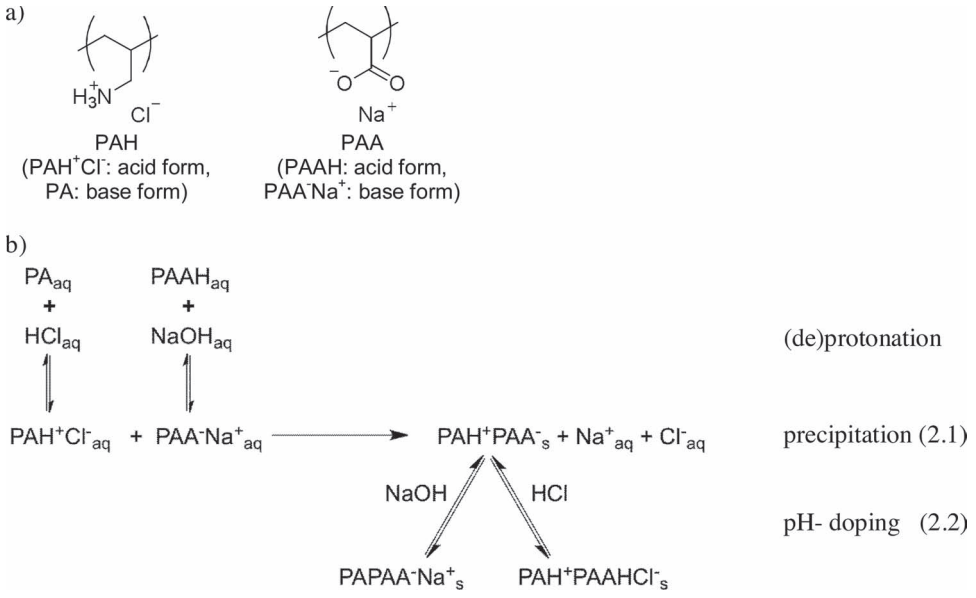

Scheme 1. a) Structures of poly(allylamine hydrochloride) (PAH) and poly(acrylic acid) (PAA) and the notations of the acid and base forms. b) Precipitation and proton doping for PAA/PAH PECs, where the uncharged forms of PAH and PAA are noted PA and PAAH, respectively, and the charged forms are noted PAH^+ and PAA^-, respectively.

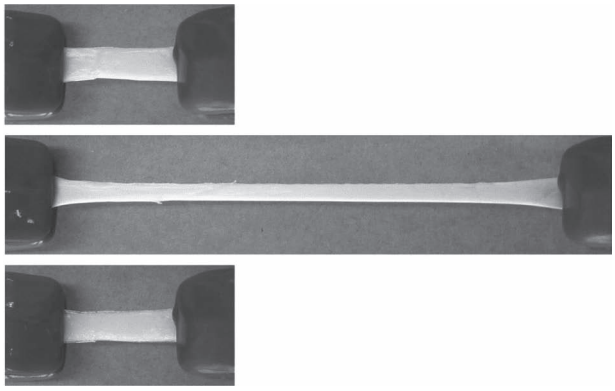

Figure 1. Stretching of an ultracentrifuged PAA/PAH complex with a PAA to PAH ratio of 1:1 conditioned in 0.15 M NaCl, pH 7.4. From top to bottom: before stretching; during stretching to 4.5 times the initial length; after 10 min the force is removed and the complex goes nearly entirely back to its original length (here, after letting it relax for 5 min). Original length of complex is 2 cm.

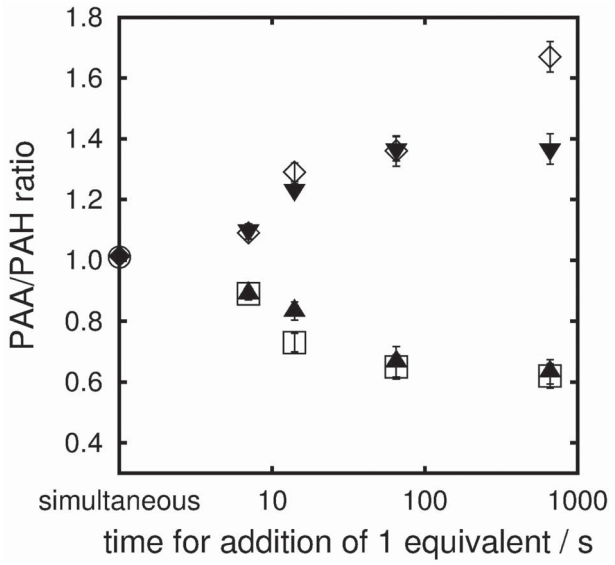

Figure 2. Influence of the speed and order of addition of the polyelectrolyte solutions on the PAA/PAH ratio in PECs at 1 M (▲ PAA in PAH, ▼ PAH in PAA, ♦ simultaneous addition) and 2.5 M NaCl (□ PAA in PAH, ◊ PAH in PAA, ○ simultaneous addition).

2.1. Preparation and Composition

Initially, the influence of several parameters on the composition of ultracentrifuged complexes of PAA and PAH was investigated. Solution ^{1}H NMR spectroscopy was used to obtain the ratio of the two polyelectrolytes in the complex: small pieces of complex were first rinsed in D_2O solutions having the same NaCl concentration and pH as the solutions used for precipitation and ultracentrifugation for 8 h in order to replace H_2O with D_2O. Complexes were then dissolved in 2.5 M NaBr in D_2O containing 0.35 M DCl. An example of a ^{1}H NMR spectrum of a dissolved complex is shown in Figure S1 (Supporting Information) together with the individual spectra of PAA and PAH under the same conditions. It can be seen that the spectra of the dissolved complexes are linear combinations of the spectra of the constituents. By comparing the intensity of the signal around 3.35 ppm (3.8–3.1 ppm), corresponding to the protons on the CH_2-group alpha to the amine group on PAH, to the broad multiplet ranging from 2.9 to 1.1 ppm corresponding to the signals from the three hydrogens on each of the backbones of PAA and PAH, the PAA to PAH ratio can be obtained using Equation 3. This approach was verified with measurements on mixtures of known amounts of PAA and PAH directly dissolved in the same solvent.

The composition of the complexes before and after ultracentrifugation varied by at most 2%. As seen in **Figure 2** the order and rate of mixing of the solutions of PAA and PAH are of prime importance for the ratio of the two polyelectrolytes in the resulting complex. The polyelectrolyte that is added to a solution of the other polyelectrolyte is always in deficit, based on the repeat units, in the resulting complex. The slower the addition, the more pronounced the deviation from 1:1 stoichiometry, though the effect levels off. The expected 1:1 pairing of charged groups to yield stoichiometric PECs of PAA and PAH is obtained when stoichiometric polyelectrolyte solutions are mixed simultaneously, as observed for mixtures of PSS and PDADMAC.[19]

The influence of mixing order and speed clearly show the importance of kinetics. When a drop of PAA (PAH) solution is added to a beaker containing PAH (PAA) solution, formation of insoluble PEC occurs immediately, and the solution becomes turbid. The PEC formed at this point has an excess of PAH (PAA), the polyelectrolyte in excess.[34] As addition continues, the concentration of solution polyelectrolyte in the beaker decreases due to PEC formation. However, the cooperativity of the interactions in the complex kinetically "freezes" the excess PAH (PAA) in the PEC, preventing access of the added PAA (PAH) to uncomplexed PAH (PAA) units. At some point all the PAH (PAA) in solution will be incorporated into PEC and further added PAA (PAH) will not produce more PEC. The resulting PEC will have an excess of PAH (PAA). In the system studied here the leveling-off of the influence of the addition speed occurred when an added drop had the time to entirely mix with the solution before a new drop was added (as could be made visible using dyes). This indicates that convection phenomena have an important influence: the faster the addition, the more the mixing resembles the mixing of equal amounts of the solutions (as in simultaneous addition) and the closer the relative concentrations of the two polyelectrolytes during this process are to 1:1.

The second major influence on the ratio was the concentration of the polyelectrolyte solutions (**Figure 3**a): For addition of PAA to PAH at a medium speed (addition of 1 equivalent in 14 s), the lower the concentration, the closer the ratio to 1:1, a trend which leveled off for high concentrations. This observation gives additional insight in how the complexes actually form. The concentration region used here is close to the expected overlap concentration of the chains (0.6 M for PAH and 0.25 M for PAA assuming ideal coil behavior).[35] At the lowest concentrations, in the dilute solution regime, complexation will take place between

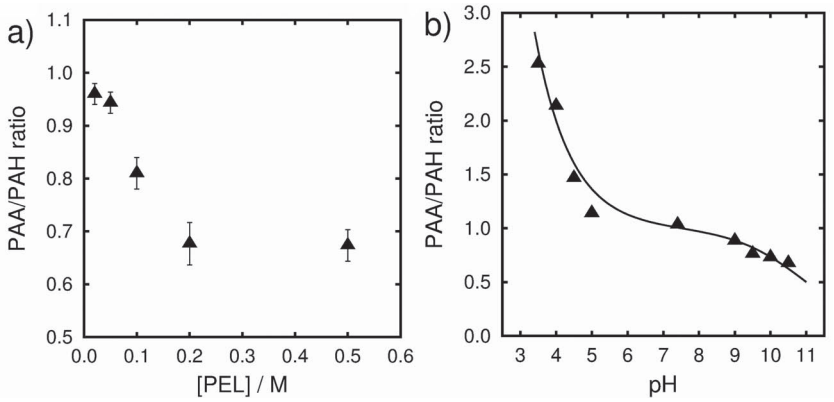

Figure 3. Influence of (a) the concentration and (b) the pH of stoichiometric polyelectrolyte solutions on the PAA/PAH ratio in ultracentrifuged complexes. a) PAA solutions of different concentrations were added to PAH solutions having the same concentrations (all in 2.5 M NaCl Tris buffer at pH 7.4). The addition time for one equivalent was 14 s. b) Complexes were obtained by adding simultaneously PAA and PAH solutions with a polyelectrolyte concentration of 0.1 M with respect to the repeat units and 0.15 M NaCl. For comparison the PAA/PAH ratio calculated from the degree of protonization obtained using the Henderson-Hasselbalch equation using a pKa of 4.0 for PAA and a pKa of 11.0 for PAH is given (solid line). Each ionized PAA unit is assumed to pair with one ionized PAH unit.

individual macromolecules, which is thought to favor intermixing at a molecular level and hence 1 to 1 pairing. The initial complexes aggregate to form well matched insoluble PECs. For higher concentrations, chain overlap occurs. An incoming PAA chain will most probably complex with several PAH chains at the same time, forming initially non-stoichiometric complexes. These will further aggregate and form inherently non-stoichiometric complexes that make charge matching difficult.

NaCl concentration (up to 2.5 M) had no major influence on the ratio of the two polyelectrolytes in the complexes (Figure 2 and Figure S2 in the Supporting Information) showing the driving force for the formation of ion-pairs between charged groups on the polyelectrolytes remains strong even in the presence of NaCl. As expected, pH on the other hand, had a strong influence on the PEC ratio due to the change of charge density of the polyelectrolytes (Figure 3b).[24,36] These experiments were carried out at a NaCl concentration of 0.15 M, which facilitated the manipulation of the very soft complexes obtained at extreme pH values. Complexes made at low pH had a significantly higher PAA content and those made at high pH a significantly lower one, consistent with PAA and PAH having reduced ionization at low pH and high pH, respectively. The ratio of PAA to PAH in the complex is expected to scale inversely with their degrees of ionization. Assuming that each ionized PAA unit interacts with each charged PAH unit, one can calculate the PAA to PAH ratio given the pKa values of both polyelectrolytes using the Henderson-Hasselbalch equation. The apparent pKa values of PAA and PAH, however, depend on the salt concentration and on the presence of the second polyelectrolyte, and they are shifted to more extreme values (lower for PAA, higher for PAH) within polyelectrolyte complexes.[24,36,37] We hence calculated this ratio for different combinations of pKa values in order to find the best fit to the experimental data. The calculated ratios using pKa values of 4.0 and 11.0 for PAA and PAH, respectively, which yields the best agreement with the experimental data assuming ideal behavior, is presented in Figure 3b (see the Supporting Information for details on the calculations and fitting). These pKa values are in good agreement with those obtained by potentiometric titration of PAA/PAH complexes (4.3/10.0 in 0.5 M NaCl, 1.9/10.7 in Milli-Q water), but deviate significantly from those obtained for the individual polyelectrolytes in solution (5.4/9.3 in 0.5 M NaCl, 6.5/8.7 in Milli-Q water).[24,36] These results indicate that the charge ratio, and therefore the polymer ratio in the complex, is strongly influenced by the polyelectrolytes already integrated within the complex having more extreme pKa values than the same polyelectrolytes in solution. This in turn suggests that under the conditions tested, either primary complexes, which formed between polyelectrolytes in solution, can reorganize while aggregating, or that a substantial part of the complexation takes place between polyelectrolytes already engaged in complexes. In both cases it would be the pKa values of the polyelectrolytes in the complex that would determine the final charge ratio and not their solution pKa values.

2.2. Porosity and Water Content

By simply changing mixing order and mixing speed it was possible to adjust the molar ratio of PAA to PAH in the complex between 0.6 and 1.4. In the next step the influence of this ratio on the properties and structure of the CoPECs was investigated, focusing on porosity, water content, and mechanical properties. Porosity and mechanical properties are important for application of these materials, and are of special interest for their use in biomedical applications. The water content of PECs is of importance in order to understand their properties and their response to environmental stimuli.

Previous studies on the PSS/PDADMA system showed that such complexes can have porosity in the micrometer range.[18] Optical microscopy of ultracentrifuged PAA/PAH complexes revealed morphological details of complexes having different PAA to PAH ratios in contact with solutions of various ionic strengths and pH values. Complexes were imaged with a fluorescence confocal microscope using their intrinsic (auto) fluorescence. PAA and PAH alone, either as powder or as concentrated solutions, also gave a signal under these conditions. The origin of this intrinsic fluorescence, which was previously attributed to aromatic groups[38] when PSS was employed in CoPECs, was unclear, although it may stem from initiator residue at chain ends. The use of confocal microscopy has the advantage that relatively thick slices can be used and no special techniques for preparation of the samples are needed. However, under physiological conditions (NaCl 0.15 M, pH 7.4) mostly used here for imaging, the complexes are not transparent and it was only possible to image the freshly cut surface while three dimensional imaging did not provide further information about the structure of these complexes.

By changing the addition order and speed, PAA/PAH CoPECs having different PAA to PAH ratios were prepared in 2.5 M NaCl and the structure of these complexes was observed after conditioning them for 24 h in 0.15 M NaCl at pH 7.4 (**Figure 4** and Figure S4–S8 in the Supporting Information). Though all these complexes were porous, the extent of the porosity, the pore size and distribution (determined through image analysis) depended strongly on the ratio of the two polyelectrolytes. The overall porosity, the mean pore size, and especially the size of the biggest pores increased as the PAA to PAH ratio approached 1. (The behavior was similar for an excess of PAA as shown in Figure S7 and Figure S8 in the Supporting Information) In particular, in the case of stoichiometric PAA/PAH complexes two distinctive populations of pores were present: large pores with diameters ranging mainly from 40 to 70 µm and numerous small pores with diameters from 5 to 15 µm. In these complexes the matrix formed a distinct membrane around the big pores, and the appearance of small pores on these membranes together with the big pores coming into contact suggest interconnectivity of the pores. While the porosity depended strongly on the ratio (it changed by a factor of 4 between CoPECs having a PAA to PAH ratio of 1 and those having a ratio of 0.6), changes in the water content with PAA to PAH ratio were less pronounced (**Figure 5**, only about 20% difference for those CoPECs). Furthermore, the stoichiometric complex showed both the highest porosity and the lowest water content in 0.15 M NaCl. The higher water content of the complexes having an excess of one of the polyelectrolytes is presumed to be due to the additional hydration water associated with the small counterions present in the complex in order to achieve charge balance. Stronger swelling was also observed for non-stoichiometric PAA/PAH multilayers.[20]

To understand what controls this variety of porosity, pore sizes, and distributions, the influence of salt concentration and ultracentrifugation was studied. For PSS/PDADMA CoPECs it was noted that the size of the pores changes with salt concentration.[18] PAA/PAH complexes were thus made and ultracentrifuged in 2.5 M NaCl and then equilibrated in solutions having different NaCl concentrations (from 0.15 to 2.5 M NaCl). The CoPECs were then sliced and imaged while in contact with the different salt solutions. Micrographs for a CoPEC having stoichiometric amounts of PAA and PAH in solutions having different NaCl concentrations are shown in **Figure 6**a. (The image in Figure 6a at 0.15 M NaCl corresponds to the one in Figure 4 bottom right obtained under the same conditions.) The large pores were hence already present in 2.5 M NaCl (the ionic strength under which these complexes were made). Small pores were not observed under these conditions, but started appearing once the NaCl concentration was lowered to about 1 M, at the same time the diameter of the larger pores increased. Decreasing the salt concentration further led to a strong increase of the number of small pores, while the size of the large ones increased only slightly. A similar effect was observed for polyelectrolyte multilayers when changing the salt concentration after film build-up.[39] For ultracentrifuged PAA/PAH complexes having a slight excess of (for example) PAH only relatively small pores were present at 2.5 M NaCl (Figure S10, Supporting Information). A decrease of the salt concentration

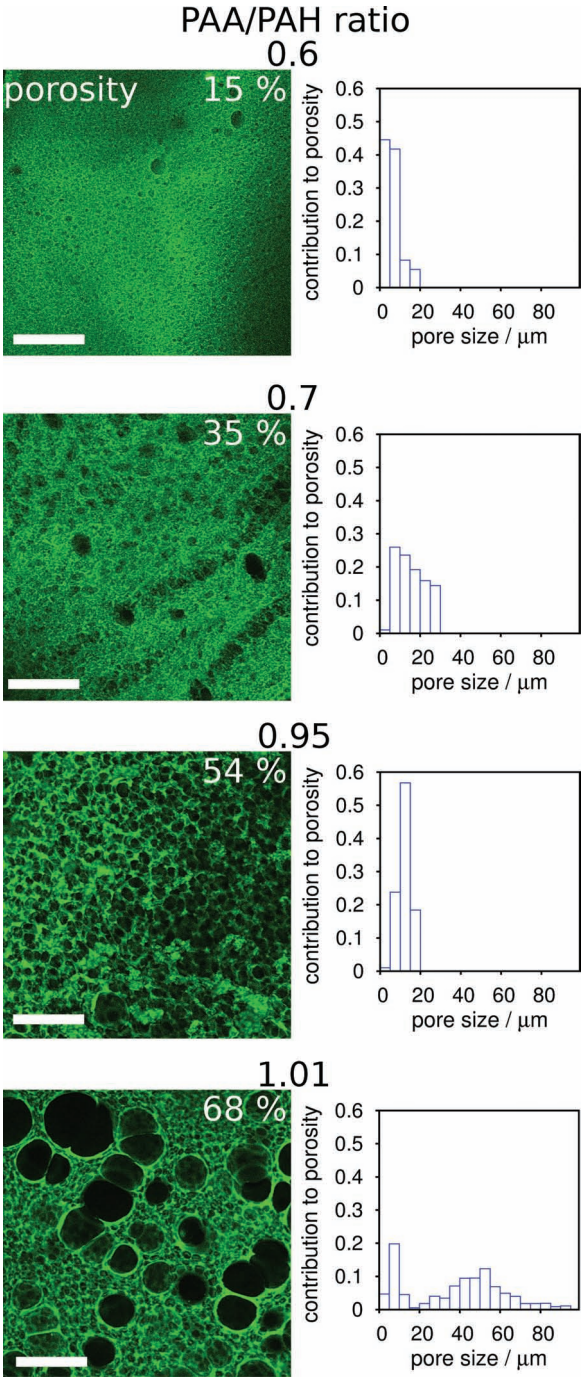

Figure 4. Influence of the PAA to PAH ratio on the microstructure of the ultracentrifuged complexes. Shown are fluorescent confocal microscopy images (λ_{ex}: 488 nm) of slices of complexes prepared in 2.5 M NaCl at pH 7.4 and conditioned in 0.15 M NaCl tris buffer at pH 7.4. Scale bars are 100 µm. The porosity is given as a percentage. Insets show how the various pore sizes contribute to the overall porosity. (Larger versions of several of these images are shown in the Supporting Information.)

led only to a slight increase in size of these, yet to a significant increase of their number.

Micrographs of stoichiometric complexes made under the same conditions but after only a short time of centrifugation

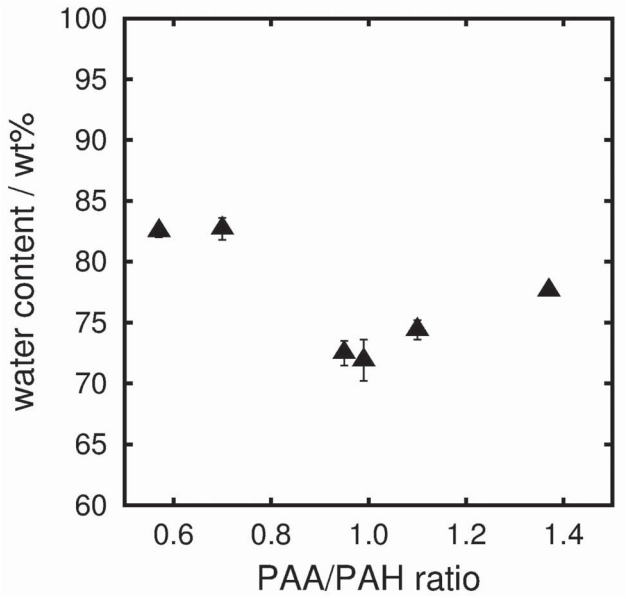

Figure 5. Influence of the PAA to PAH ratio of ultracentrifuged complexes prepared in 2.5 M NaCl on their water content at 0.15 M NaCl, pH 7.4.

at low speed (Figure S9, Supporting Information) showed that before ultracentrifugation the large pores are substantially larger, reaching up to more than 200 µm. It is imagined that these pores are formed when primary complexes that precipitate from solution stick together. As the pieces do not pack perfectly together, voids appear. During ultracentrifugation the complexes are homogenized under the action of the centrifugal field. However, this homogenization is not complete and the voids are not entirely closed due to the low mobility of the polyelectrolytes. As will be shown below the mobility of the polyelectrolytes was lowest in the stoichiometric complexes, thus the biggest voids remain in these complexes. Smaller defects might also be present in the complexes. When the ionic strength is decreased the pore sizes increased up to a maximum size about twice the size they had at the conditions used for precipitation and ultracentrifugation (2.5 M NaCl). The overall size increase is strongest for the stoichiometric complex. In this case small pores, that could stem from small defects in the complex, appear at low ionic strength.

On a macroscopic level the complexes swell with decreasing salt concentration as can also be seen from the increase of the water content. For the case of the stoichiometric complex this is shown in Figure 6b. However, the swelling is less than would be expected from the increase of the porosity. This means that the matrix actually shrinks with decreasing salt concentration as would be expected for a stoichiometric PEC.[4,19] This behavior was also observed for PAA/PAH multilayers. In 0.15 M NaCl a stoichiometric PAA/PAH CoPEC contained about 73% water predominantly located in the pores (porosity 68%). The remaining water is assumed to be hydration water of the matrix, giving a water content of the matrix around 15 to 20%, which is in good agreement with the hydration measured for PAA/PAH multilayers.[5,20] While the matrix itself shrunk, and the pores grew with decreasing ionic strength, the complex

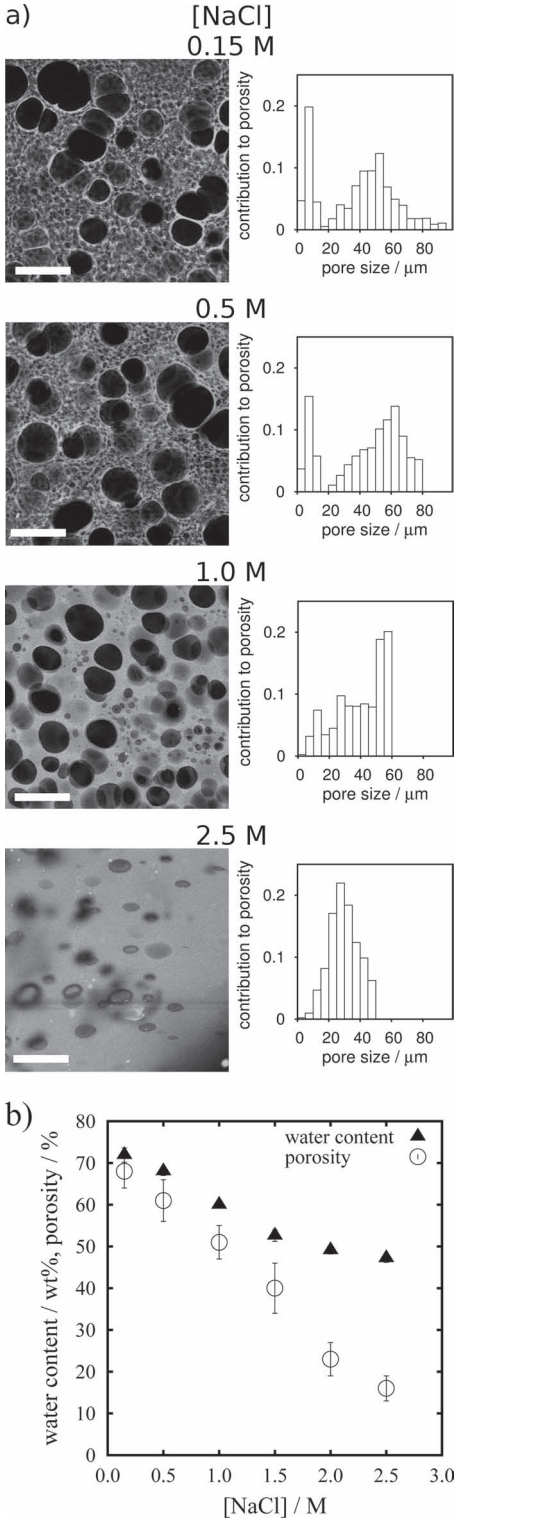

Figure 6. Influence of the salt concentration on the microstructure, the porosity, and the water content of ultracentrifuged complexes prepared at 2.5 M NaCl, pH 7.4 having a PAA to PAH ratio of 1:1. a) Shown are fluorescent microscopy images (λ_{ex}: 488 nm) of slices of complexes conditioned in solutions at pH 7.4 having different concentrations of NaCl. Scale bars are 100 µm. b) Water content and porosity obtained under the same conditions.

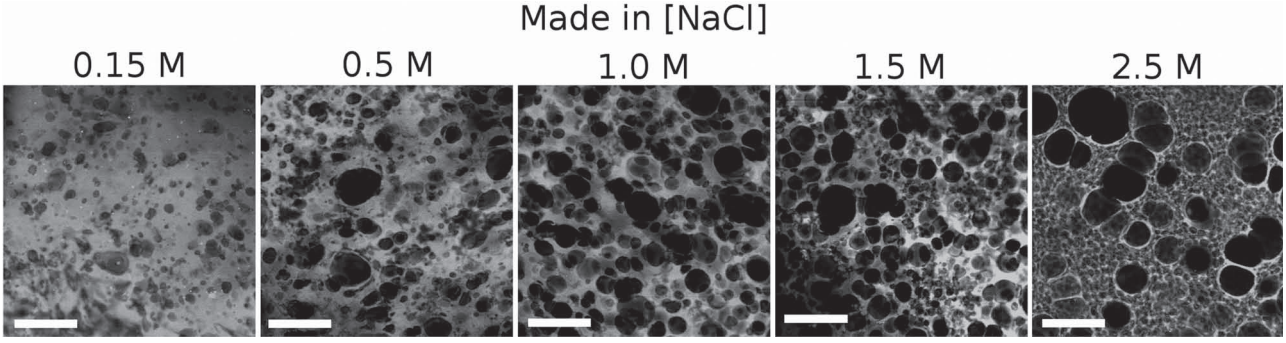

Figure 7. Influence of the salt concentration during preparation on the microstructure of 1:1 ultracentrifuged complexes equilibrated in 0.15 M NaCl, pH 7.4. Shown are fluorescent microscopy images (λ_{ex}: 488 nm) of slices of complexes made from polyelectrolyte solutions having different concentrations of NaCl and ultracentrifuged under these conditions. The complexes were then all conditioned in 0.15 M NaCl at pH 7.4. Scale bars are 100 μm.

swelled on a macroscopic scale due to the increased osmotic pressure probably exerted by domains of non-stoichiometric complex located on the walls of the pores.[40] Together with the voids and inhomogeneities remaining after ultracentrifugation shrinking of the matrix at low salt concentration leads to the observed porosity and pore size distributions.

Porosity, pore size, and distribution depended on the ratio of the polyelectrolytes and the ionic strength, or more precisely on the difference in the ionic strength at which the complex was made. This can be employed in several ways to tune the porosity. Varying the ratio of PAA to PAH as discussed above through the precipitation conditions is a first example. Changing the salt concentration of a solution in contact with the complex is a second possibility, and an example of the inherent responsiveness of these materials to external stimuli. In a third approach we made stoichiometric complexes from solutions containing different amounts of salt (**Figure 7**). When these were conditioned in 0.15 M NaCl after the ultracentrifugation the pores depended on the NaCl concentration at which the complex was made. A complex made in 1.5 M NaCl showed two distinct populations of pores similar to those in the complex made at 2.5 M NaCl, yet smaller. If the complex was made in 1 M NaCl no small pores appeared, while a large number of large pores was present. Further decrease of the ionic strength during precipitation led, however, to less uniform patterns of porosity. This is due on the one hand to the fact that the change in ionic strength is not sufficient to swell the pores significantly and on the other hand to less effective homogenization during ultracentrifugation at these lower salt concentrations. At the same time the water content (at a given NaCl concentration, e.g., 0.15 M) changed also with the salt concentration at which the complexes were made (Figure S11, Supporting Information).

The importance of the PAA to PAH ratio in determining the structure and properties of these complexes lies in its influence on charge compensation between charges on the polyelectrolytes. Excess charge on one of the polyelectrolytes leads to charge compensation by small counter ions and hence to increased hydration and swelling of the matrix.[24] In the case of PAA and PAH that bear respectively weak acid and weak basic groups, this charge balance can also be influenced through the pH (see Scheme 1). As shown in **Figure 8**, this could effectively be used as a further way to control the porosity of the materials and shows the responsiveness of these complexes to pH.

Together, these results show that it is possible to create materials with a wide variety of porosities, and pore sizes and distributions by only changing the mixing conditions of two polyelectrolyte solutions, and to control the porosity by external stimuli such as salt concentration or pH.

2.3. Mechanical Properties

The mechanical properties and the way in which these are influenced by the PAA to PAH ratio in the ultracentrifuged complexes were studied using rheology. In particular, we studied the response of the complexes to shear stress and the frequency dependence of the storage and loss moduli G′ and G″, and of

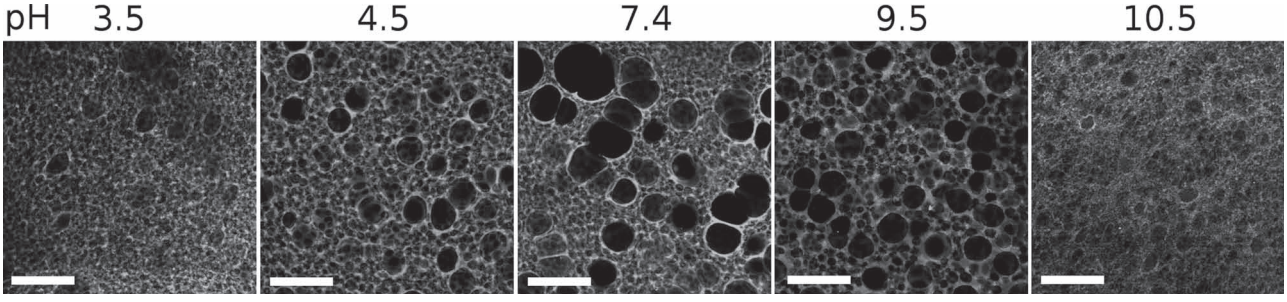

Figure 8. Influence of the pH on the microstructure of 1:1 ultracentrifuged complexes prepared at 2.5 M NaCl, pH 7.4. Shown are fluorescent microscopy images (λ_{ex}: 488 nm) of slices of complexes conditioned in 0.15 M NaCl solutions at different pH values. Scale bars are 100 μm.

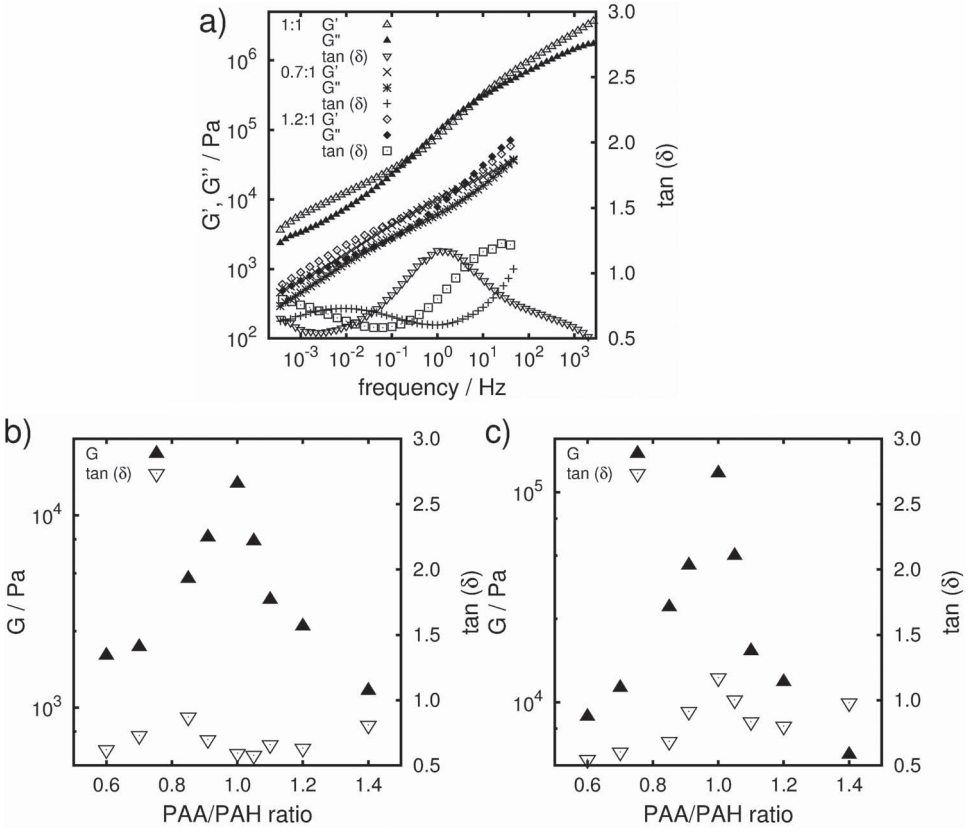

Figure 9. a) Frequency dependence of G′, G″, and tan (δ) for ultracentrifuged complexes having different PAA to PAH ratios in 0.15 M NaCl, pH 7.4. b,c) G and tan (δ) at (b) 0.01 and (c) 1 Hz depending on the PAA to PAH ratio under the same conditions.

tan (δ) on disks of the complexes using a plate-plate geometry in a fixed stress rheometer and a piezorheometer working with fixed strain for the highest frequencies. The PEC samples were conditioned in 0.15 M NaCl at pH 7.4 for at least 24 h before the measurements. Results for complexes having stoichiometric amounts of PAA and PAH and either a large PAA or PAH excess are shown in **Figure 9**a. Data from overlapping frequency ranges using the rheometer and the piezorheometer were identical within 3%.

For the stoichiometric CoPEC G′ and G″ showed a relaxation behavior over the whole frequency domain studied here. In view of the extent of the frequency range (8 decades) this cannot be explained by a single relaxation mechanism. In particular 3 distinct regions can be differentiated: At low frequencies G′ is superior to G″ indicating a gel-like behavior. This is associated with the physical cross-links formed by ion-pairs between positive and negative groups on PAH and PAA, respectively. However, the fact that a distinct elastic plateau is not observed suggests the presence of additional types of relaxation. Such relaxations could be attributed to the presence of pores, and more precisely to the presence of polyelectrolytes in the pores and on the walls of the pores exerting an osmotic pressure and an additional viscous component to the behavior of the CoPECs.[18] At intermediate frequencies a marked viscoelastic behavior was observed with G′ and G″ being of similar magnitude and increasing roughly in parallel. At the same time the phase angle passes through a maximum. This behavior is associated with the relaxations of the polymer chains forming the gel. In the high frequency region both G′ and G″ increase with increasing frequency, though the increase of G′ dominates. This reflects the progressive freezing of intrachain molecular relaxations with increasing frequency. Such a behavior is characteristic for the transition zone preceding glassy behavior. However, the glassy plateau is not reached within the frequency region studied. The general behavior of PAA/PAH CoPECs resembles hence the one of PSS/PDADMA CoPECs with the major difference being the absence of a marked "saloplastic" plateau.[17]

For complexes having an excess of one of the polyelectrolytes the curves seemed to be shifted to higher frequencies (though a superposition is not possible) and the gel-like behavior was still less expressed (see Figure S12 in the Supporting Information for the curves corresponding to different ratios). Accordingly, both G′ and G″ at a given frequency decreased strongly with increasing deviation from stoichiometry. This corresponds to the complexes becoming softer. In Figure 9b and Figure 9c the shear modulus G, corresponding to $(G'^2 + G''^2)^{0.5}$ and tan (δ) at two frequencies (0.01 and 1 Hz) are shown for various PAA to PAH ratios. The closer the ratio is to 1: 1, the stiffer were the resulting materials. This is somewhat surprising as this also corresponds to them being the most porous. However, the rigidity of polymeric materials increases with the density of cross-links,[41,42] and a 1 to 1 matching of the charges

on the polyelectrolytes yields the highest density of cross-links. Furthermore, we have seen (Figure 5) that the water content is actually lowest in stoichiometric complexes, which further increases the overall cross-link density. Together these explain the strong increase in modulus for stoichiometric complexes. The observed modulus for stoichiometric complexes even at the highest frequencies measured here (shear modulus around 4 MPa, corresponding to a Young's modulus of 12 MPa) is still significantly lower than those reported for PAA/PAH multilayers, for which Young's moduli of the order of 70 MPa were found.[43] A direct comparison is, however, difficult, as we performed our measurements at finite frequencies. Apart from this, the high porosity of the complexes investigated here may contribute to this difference. If the salt concentration is lowered, the complexes became stiffer (Figure S13, Supporting Information), with the curves being shifted to lower frequencies. This is due to a decrease in the doping level (Equation 1.2), leading to an increase of the cross-link density.

The maximum of tan (δ) for the stoichiometric CoPEC lies close to 1 Hz, corresponding to the transition region between the gel-like behavior and the onset of the freezing of the molecular movements. Tan (δ) at this frequency decreases with increasing non-stoichiometry corresponding to the gel-like behavior being displaced to higher frequencies (Figure 9). The relatively high tan (δ) for the CoPEC having the highest excess of PAA indicates its liquid-like behavior. At 0.01 Hz the tan (δ) of the stoichiometric CoPEC is lowest, indicating that its behavior is the most elastic and solid like due to the high density of ionic cross links. CoPECs with PAA to PAH ratio significantly different from 1 to 1 show a more liquid like behavior and thus flow more easily. This increased mobility of the polyelectrolyte chains in turn is assumed to lead to a better homogenization of the complexes during ultracentrifugation.

The ultracentrifuged PAA/PAH complexes also showed excellent resistance to stretching, and, for example, the stoichiometric complex in 0.15 M NaCl could be stretched to more than 6 times its original length before breaking. When stretched to 4.5 times its original length the complex recovered nearly entirely its original length when the stress was released, though this took about 10 min (Figure 1).

3. Conclusions

In this work we showed that the approach for compaction of polyelectrolyte complexes by ultracentrifugation can not only be applied to strong polyelectrolytes (PSS/PDADMA) but also to couples of weak polyelectrolytes, in this case PAA and PAH. In this way macroscopically homogeneous, yet porous materials showing good mechanical resistance and elasticity under physiological conditions were obtained. By simply changing the mixing conditions, composition, porosity, and mechanical properties could be controlled over a wide range. These materials are furthermore responsive both to salt concentration and pH, allowing for a fine tuning of their structure.

Previous studies of polyelectrolyte multilayers composed of PAA and PAH have shown their potential for biomedical applications. Together with the possibilities to control their three dimensional structure and their mechanical properties shown here, this makes compact complexes of PAA and PAH excellent candidates for biomaterials, such as scaffolds for tissue engineering applications.

4. Experimental Section

Materials: Poly(acrylic acid) (PAA, Sigma-Aldrich, M_w 250 000 g/mol) and poly(allyl amine hydrochloride) (PAH, AlfaAesar, M_n 40 000 g/mol, M_w 104 000 g/mol) were dissolved in water, dialyzed for 2 days against water, neutralized, and lyophilized. NaCl (>99%, Carlo Erba), tris(hydroxy)methyl aminomethane (Tris base, 99.96%, Euromedex), acetic acid (>99.8%, Sigma-Aldrich), ethanolamine (98+%, Alfa Aesar), DCl (99 atom% D, Sigma-Aldrich), D_2O (99.9 atom% D, Eurisotop), and KBr (99+%, Acros) were used as received. 18 MΩ Milli-Q-water (Millipore) was used in all experiments.

Complexes: PAA/PAH polyelectrolyte complexes were precipitated by mixing aqueous solutions of PAA and PAH. Mixing was performed by adding either one solution to a beaker containing the other solution or by simultaneously pumping both solutions into one beaker using a peristaltic pump (Ismatec) at various flow rates. Reactions were stirred with a magnetic stirbar at 200 rpm. The polyelectrolyte concentration, NaCl concentration, and pH were varied during the study. Buffers were 10 mM in Tris, acetate, or ethanolamine, respectively. When used as a variable, pH was adjusted over a wide range in 0.15 M NaCl.

Complexes were transferred into polycarbonate thick-wall centrifuge tubes (Beckman Coulter Inc.) with their supernatant and ultracentrifuged in a Beckman Coulter Ultracentrifuge using a Ti90 rotor at 188 000g for 4 h at 23 °C.

NMR Spectroscopy: Proton NMR spectroscopy (Bruker Avance 400 MHz spectrometer) was used to measure the ratio of PAA to PAH in the complexes as follows: excess solution was removed from a piece of complex (20–30 mg) using paper wipes. To exchange most of the hydration H_2O with D_2O the complex was rinsed with 1 M NaCl in D_2O (in three 0.5 mL aliquots over 8 h). The piece of complex was then dissolved in 0.5 mL of a D_2O solution containing 2.5 M KBr and 0.35 M DCl. The ratio of PAA to PAH in the complex was obtained by comparison of the intensity of the signal around 3.35 ppm (corresponding to the hydrogens on the CH_2-group alpha to the amine group) to the remaining signal:

$$\frac{\mathrm{PAA}}{\mathrm{PAH}} = \frac{I_{(1.1-2.9\ \mathrm{ppm})} - 1.5 \cdot I_{(3.1-3.8\ \mathrm{ppm})}}{1.5 \cdot I_{(3.1-3.8\ \mathrm{ppm})}} \quad (3)$$

(See Figure S1 in the Supporting Information for the corresponding spectra.) For calibration, spectra of mixtures of known amounts of PAA and PAH in the same solvent were recorded. Chemical shifts are given relative to the water signal set to 4.79 ppm.

Water Content: Complexes were equilibrated under the desired conditions, then dried at 80 °C for 72 h. Weighing the complexes before and after drying yielded an estimate of the water content.

Microscopy: Slices of complexes equilibrated under the desired conditions were obtained by rapidly freezing them in liquid nitrogen and slicing them using histological blades. The slices were stored in the corresponding buffer solutions.

Fluorescence microscopy images were obtained on a Zeiss LSM confocal microscope using a 10× objective with excitation at 488 nm. The autofluorescence of the polyelectrolytes was used for imaging. Pore sizes and porosities were determined using the ImageJ software.[44] For the determination of the porosity parts of the images (200 µm × 200 µm) were transformed into binary images, from which the porosity could be obtained. Three distinct regions of three different images were used for each condition. The pore sizes were obtained by using the integrated routines for the analysis of particles. These results were confirmed by manually measuring the diameters of the pores on parts of the images. The obtained pore sizes thus correspond to the sizes of their projections, which hence underestimate the actual pore diameters.[45,46]

However, they should be adequate for the comparison of the pore sizes under different conditions.

Rheology: For mechanical testing, freshly ultracentrifuged complexes were compressed in 2.5 M NaCl between two plates separated by a 1 mm spacer for 1 h then transferred first into Tris buffer containing 0.15 M NaCl at pH 7.4, then into the desired solutions. The ca. 1-mm-thick sheets were cut into disks of diameter 35 mm and their thickness was measured. The disks were kept in the buffer until testing.

To characterize the mechanical behavior of ultracentrifuged polyelectrolyte complexes on an extended frequency range, shear measurements made with a conventional rheometer operating at fixed stress (Haake Rheowin Rheometer, Fisher Scientific) were supplemented by shear measurements performed with a piezorheometer. All tests were performed in a plate-plate geometry with the sample in contact with the corresponding solutions (typically 0.15 M NaCl, 10 mM Tris, pH 7.4). For measurements using the classical rheometer, especially suited for measurements at low frequencies, preliminary tests were performed to determine the suitable stress for operating in the linear viscoelastic regime. The piezorheometer on the other hand allows one to acquire data in a range of frequency (up to a few kHz), inaccessible to classical rheometers. This apparatus is a plate-plate strain rheometer that uses piezoelectric ceramics vibrating in the shear mode. A detailed description can be found in references.[47,48] For the samples studied here, shear measurements were performed at 25 °C for frequencies ranging from 10^{-1} Hz to 3 kHz. The applied strain, ε, was very low ($\varepsilon \approx 10^{-5}$) and the validity of the linear response was checked experimentally.

Supporting Information

Supporting Information is available from the Wiley Online Library or from the author.

Acknowledgements

This work was supported by the Gutenberg Chair program of the Université de Strasbourg and by the ANR (grant BIOSTRETCH ANR-10-BLAN-0818). We gratefully acknowledge Joseph Hemmerlé and Karim Benmlih for the design of the devices used for the preparation of the samples for mechanical testing, Joseph Selb for his help with the rheology experiments, as well as Mélanie Legros and Odile Gavat for the GPC analysis.

Received: May 25, 2012
Revised: August 20, 2012
Published online: September 20, 2012

[1] R. Gentsch, H. Börner, *Adv. Polym. Sci.* **2011**, *240*, 163.
[2] A. S. Michaels, H. J. Bixler, *Encycl. Chem. Technol.* **1968**, *16*, 117.
[3] C. B. Bucur, Z. Sui, J. B. Schlenoff, *J. Am. Chem. Soc.* **2006**, *128*, 13690.
[4] J. B. Schlenoff, A. H. Rmaile, C. B. Bucur, *J. Am. Chem. Soc.* **2008**, *130*, 13589.
[5] S. T. Dubas, J. B. Schlenoff, *Langmuir* **2001**, *17*, 7725.
[6] D. W. Pack, A. S. Hoffman, S. Pun, P. S. Stayton, *Nat. Rev. Drug Discovery* **2005**, *4*, 581.
[7] C. Schmitt, C. Sanchez, S. Desobry-Banon, J. Hardy, *Crit. Rev. Food Sci. Nutr.* **1998**, *38*, 689.
[8] I. K. Voets, A. D. Keizer, M. A. C. Stuart, *Adv. Colloid Interface Sci.* **2009**, *147–148*, 300.
[9] G. Decher, *Science* **1997**, *277*, 1232.
[10] P. T. Hammond, *Adv. Mater.* **2004**, *16*, 1271.
[11] Z. Tang, Y. Wang, P. Podsiadlo, N. A. Kotov, *Adv. Mater.* **2006**, *18*, 3203.
[12] E. Leguen, A. Chassepot, G. Decher, P. Schaaf, J. Voegel, N. Jessel, *Biomol. Eng.* **2007**, *24*, 33.
[13] P. Lavalle, J. C. Voegel, D. Vautier, B. Senger, P. Schaaf, V. Ball, *Adv. Mater.* **2011**, *23*, 1191.
[14] D. Mertz, C. Vogt, J. Hemmerle, J. Mutterer, V. Ball, J. Voegel, P. Schaaf, P. Lavalle, *Nat. Mater.* **2009**, *8*, 731.
[15] A. S. Michaels, R. G. Miekka, *J. Phys. Chem.* **1961**, *65*, 1765.
[16] A. S. Michaels, *Ind. Eng. Chem.* **1965**, *57*, 32.
[17] C. H. Porcel, J. B. Schlenoff, *Biomacromolecules* **2009**, *10*, 2968.
[18] H. H. Hariri, J. B. Schlenoff, *Macromolecules* **2010**, *43*, 8656.
[19] R. F. Shamoun, A. Reisch, J. B. Schlenoff, *Adv. Funct. Mater.* **2012**, *22*, 1923.
[20] J. D. Mendelsohn, S. Y. Yang, J. Hiller, A. I. Hochbaum, M. F. Rubner, *Biomacromolecules* **2003**, *4*, 96.
[21] J. A. Lichter, M. F. Rubner, *Langmuir* **2009**, *25*, 7686.
[22] J. A. Lichter, M. T. Thompson, M. Delgadillo, T. Nishikawa, M. F. Rubner, K. J. Van Vliet, *Biomacromolecules* **2008**, *9*, 1571.
[23] J. Hiller, M. F. Rubner, *Macromolecules* **2003**, *36*, 4078.
[24] J. Choi, M. F. Rubner, *Macromolecules* **2005**, *38*, 116.
[25] A. J. Chung, M. F. Rubner, *Langmuir* **2002**, *18*, 1176.
[26] L. A. Connal, Q. I. Li, J. F. Quinn, E. Tjipto, F. Caruso, G. G. Qiao, *Macromolecules* **2008**, *41*, 2620.
[27] D. E. Discher, D. J. Mooney, P. W. Zandstra, *Science* **2009**, *324*, **1673**.
[28] J. D. Mendelsohn, C. J. Barrett, V. V. Chan, A. J. Pal, A. M. Mayes, M. F. Rubner, *Langmuir* **2000**, *16*, 5017.
[29] Y. S. Nam, T. G. Park, *J. Biomed. Mater. Res.* **1999**, *47*, 8.
[30] V. Karageorgiou, D. Kaplan, *Biomaterials* **2005**, *26*, 5474.
[31] E. Chevalier, D. Chulia, C. Pouget, M. Viana, *J. Pharm. Sci.* **2008**, *97*, 1135.
[32] V. A. Kabanov, *Russ. Chem. Rev.* **2005**, *1*, 3.
[33] J. B. Schlenoff, S. T. Dubas, *Macromolecules* **2001**, *34*, 592.
[34] N. Karibyants, H. Dautzenberg, H. Cölfen, *Macromolecules* **1997**, *30*, 7803.
[35] Q. Ying, B. Chu, *Macromolecules* **1987**, *20*, 362.
[36] A. I. Petrov, A. A. Antipov, G. B. Sukhorukov, *Macromolecules* **2003**, *36*, 10079.
[37] H. H. Rmaile, J. B. Schlenoff, *Langmuir* **2002**, *18*, 8263.
[38] M. G. Neumann, G. L. de Sena, *Colloid Polym. Sci.* **1999**, *277*, 414.
[39] H. Mjahed, G. Cado, F. Boulmedais, B. Senger, P. Schaaf, V. Ball, J. Voegel, *J. Mater. Chem.* **2011**, *21*, 8416.
[40] M. Z. Markarian, H. H. Hariri, A. Reisch, V. S. Urban, J. B. Schlenoff, *Macromolecules* **2012**, *45*, 1016.
[41] J. A. Jaber, J. B. Schlenoff, *J. Am. Chem. Soc.* **2006**, *128*, 2940.
[42] L. R. G. Treloar, *The Physics of Rubber Elasticity*, Clarendon, Oxford **1975**.
[43] A. M. Lehaf, M. D. Moussallem, J. B. Schlenoff, *Langmuir* **2011**, *27*, 4756
[44] W. S. Rasband, ImageJ, U. S. National Institutes of Health, Bethesda, Maryland, USA, 1997–2012.
[45] K. Wiencek, T. Skowronek, B. Khatemi, *Metall. Foundry Eng.* **2005**, *31*, 167.
[46] ASTM E112, "Standard Test Methods for Determining Average Grain Size", ASTM International, West Conshohocken, PA, **2004**, DOI: 10.1520/E0112-96R04.
[47] O. Pozo, D. Collin, H. Finkelmann, D. Rogez, P. Martinoty, *Phys. Rev. E* **2009**, *80*, 031801.
[48] D. Collin, P. Lavalle, J. M. Garza, J. Voegel, P. Schaaf, P. Martinoty, *Macromolecules* **2004**, *37*, 10195.